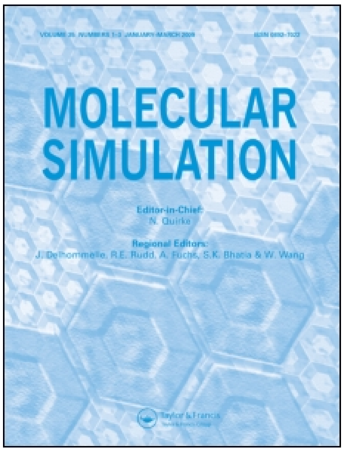

Molecular Simulation
Publication details, including instructions for authors and subscription information:
http://www.informaworld.com/smpp/title~content=t713644482

Thermal-stability and tensile properties of two single-walled Si-H nanotubes

H. Shen[a]
[a] School of Aeronautics & Astronautics, Nanjing University of Aeronautics & Astronautics, Nanjing, P. R. China

To cite this Article Shen, H.(2007) 'Thermal-stability and tensile properties of two single-walled Si-H nanotubes', Molecular Simulation, 33: 11, 939 — 944
To link to this Article: DOI: 10.1080/08927020701502016
URL: http://dx.doi.org/10.1080/08927020701502016

Molecular Simulation, Vol. 33, No. 11, September 2007, 939–944

Taylor & Francis
Taylor & Francis Group

Thermal-stability and tensile properties of two single-walled Si—H nanotubes

H. SHEN*

School of Aeronautics & Astronautics, Nanjing University of Aeronautics & Astronautics, Nanjing 210016, P. R. China

(Received December 2006; in final form June 2007)

The Molecular dynamics (MD) method was used to predict the thermal-stability and tensile properties of two single-walled Si nanotubes that are hydrogenated outside and both inside and outside respectively, i.e. the Si_o—H and Si_{io}—H nanotubes. Further, the axial-tensile properties of the two Si—H nanotubes were discussed by comparison with one (14,14) carbon nanotube. The obtained results show that: (1) the two Si—H nanotubes both have the Si skeletons with the structure similar to the {110} planes of single-crystal silicon, and they can stably exist only at the temperature lower than 200 and 125 K respectively and (2) the Si_o—H and Si_{io}—H nanotubes, respectively, have the tensile strength of 4.0 and 1.2 GPa as well as the fracture strain of 0.35 and 0.32; both their tensile strength and fracture strain are much lower than the corresponding ones of the (14,14) carbon-tube.

Keywords: Si—H nanotubes; Thermal-stability; Tensile properties; Molecular dynamics

1. Introduction

Since, carbon nanotube (CNT) was found in 1991, it has attracted tremendous attentions from physicists, chemists and material designers due to its excellent electronic and mechanical properties [1,2]. In the element periodic table Si and C, as the IV-group elements, have similar electronic structure, so researchers hope to be able to obtain the single-walled Si nanotubes with the configuration similar to CNT [3–5]. Recently Tang *et al.* reported multi-walled Si nanotubes [6], but it is found that the Si nanotubes have the walls of the diamond-like sp^3-structure, and that the spacing between the adjacent walls is about 0.31 nm, just corresponding to that between the {110} planes of single-crystal silicon (SCS). What's the reason? It is ascribed to the fact that silicon with the sp^3-structure has much lower energy than that with the sp^2-structure [7–9]. However, the authors of Refs. [3,5] put forwards one assumption about the single-walled Si nanotubes. It is thought that single-walled Si nanotubes with stable sp^3-structure is likely to be obtained by hydrogenating the sp^2-structure Si nanotubes outside or inside, which provides a new idea for the preparation of single-walled Si nanotube.

Silicon is the most important material for micro/nano-electronic applications, and it is undoubtedly significant to predict the physical properties of Si nanotubes. Now the theoretical researches about the micro-structures and electronic properties of the single-walled Si-tubes and the single-walled hydrogenated Si-tubes, i.e. the single-walled Si—H nanotubes, have been carried out [3–5], but the thermal-stability and mechanical properties of the single-walled Si—H nanotubes have not been reported up to now. Considering the reason, with two single-walled Si nanotubes, hydrogenated outside and both inside and outside and called as Si_o—H and Si_{io}—H nanotubes respectively, as investigated objects, the MD simulations are performed to study their thermal-stability and tensile properties. Further, according to the simulated results, their differences in thermal-stability and tensile properties are discussed. Some conclusions in the present paper are helpful for researchers to further recognize the physical properties of the single-walled Si—H nanotubes.

2. Model and method

2.1 *The investigated objects*

Figure 1 shows the investigated objects, one single-walled Si_o—H nanotube and one single-walled Si_{io}—H nanotube. Both the two Si—H nanotubes have 660 silicon atoms and

---

*Corresponding author. Tel.: + 86-25-84896252. Email: shj@nuaa.edu.cn

Molecular Simulation
ISSN 0892-7022 print/ISSN 1029-0435 online
http://www.tandf.co.uk/journals
DOI: 10.1080/08927020701502016

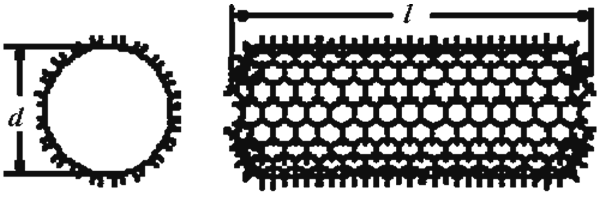

(a) The Si_o-H nanotube

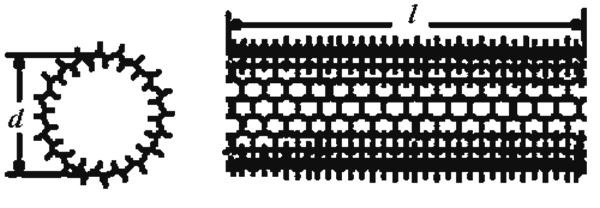

(b) The Si_{io}-H nanotube

Figure 1. The Si_o—H and The Si_{io}—H nanotubes.

700 hydrogen atoms. The models of the Si_o—H and Si_{io}—H nanotubes are constructed by the following method: first, using CNT "generator", a computer-program developed by us [2], to get two (10,10) CNTs; secondly, replacing all the carbon atoms of the two (10,10) carbon-tubes with silicon atoms to get two silicon nanotubes, i.e. the Si skeletons of the Si_o—H and Si_{io}—H nanotubes; then "hydrogenating" all the Si atoms of one silicon-tube outside to get the Si_o—H nanotube and hydrogenising the Si atoms of another silicon-tube alternately inside and outside to get the Si_{io}—H nanotube; at last, geometrically optimizing the two Si—H nanotubes and obtaining their initial configures, see figure 1. Here the modeling and geometrical optimization of the Si—H nanotubes are performed in the famous quantum-chemical software of HyperChem 7® [10]. In the optimizations the MM + force-field, the conjugate gradient method by Fletcher *et al.* [11], and the convergence limit of 0.01 kcal/mol are taken. The optimized Si_o—H and Si_{io}—H tubes both have the length l about 5.7 nm and the diameter d about 2.12 nm. In the two Si—H tubes the Si—Si bondings are about 0.237 nm long and the Si—H bondings about 0.148 nm.

2.2 Simulation details

In this paper the classical MD simulations are performed to investigate the thermal-stability and tensile properties of two Si—H nanotubes. In MD, the time evolution of interacting atoms is followed by integrating their equations of motion, which can help people to comprehend more details of matter motion at atomic level. Generally speaking, many-body potentials can more accurately describe the interactions between atoms than simple pair-potentials. Of the available many-body potentials, Tersoff potential, a famous bond order potential derived from quantum-mechanical arguments, can well consider bond order and covalent bonds forming/breaking for the systems of C, Si, H and so on and has been widely used to calculate the bonding energy, micro-structure, melting and volume module for the materials of hydrogen and the IV-group elements [12–16]. So the Tersoff potential is adopted to simulate the melting and tension of the Si—H and C nanotubes here. For the interactions between two neighbouring atoms i and j, the form of the energy Φ is taken to be

$$\Phi = \sum_{i}\sum_{j>i} f_c[a_{ij}\cdot E_r(r_{ij}) - b_{ij}\cdot E_a(r_{ij})] \tag{1}$$

with

$$\begin{aligned} E_r(r_{ij}) &= A_{ij}\cdot \exp(-\lambda_{ij}\cdot r_{ij}) \\ E_a(r_{ij}) &= B_{ij}\cdot \exp(-\mu_{ij}\cdot r_{ij}) \\ f_c(r_{ij}) &= \begin{cases} 1 & r_{ij} < R_{ij} \\ \frac{1}{2}\left[1+\cos\left(\pi\frac{r_{ij}-R_{ij}}{S_{ij}-R_{ij}}\right)\right] & R_{ij} < r_{ij} < S_{ij} \\ 0 & S_{ij} < r_{ij} \end{cases} \end{aligned} \tag{2}$$

b_{ij} is the many-body order parameter describing how the bond-formation energy is affected by the local atomic arrangement due to the presence of other neighbouring atoms (the k-atoms). It is a many-body function of the positions of the atoms i, j and k. It has the form of

$$b_{ij} = \chi_{ij}\left(1+\beta_i^{n_i}\cdot\xi_{ij}^{n_i}\right)^{-(m_i/2n_i)} \tag{3}$$

with

$$\xi_{ij} = \sum_{k\neq i,j} f_c(r_{ik})\omega_{ik}\cdot g(\theta_{ijk})$$

$$g(\theta_{ijk}) = 1 + \frac{c_i^2}{d_i^2} - \frac{c_i^2}{d_i^2 + (h_i + \cos\theta_{ijk})^2}$$

$$a_{ij} = \varepsilon_{ij}\left(1+\beta_i^{n_i}\cdot\tau_{ij}^{n_i}\right)^{(-1/2n_i)}$$

$$\tau_{ij} = \sum_{k\neq i,j} f_c(r_{ij})\delta_{ik}\cdot g(\theta_{ijk})$$

$$\lambda_{ij} = \frac{\lambda_i + \lambda_j}{2} \tag{4}$$

$$\mu_{ij} = \frac{\mu_i + \mu_j}{2} \tag{5}$$

$$A_{ij} = \sqrt{A_i A_j} \tag{6}$$

$$B_{ij} = \sqrt{B_i B_j} \tag{7}$$

where, r_{ij} is the distance of the i th and j th atom, θ_{ijk} is the angle between r_{ij} and r_{jk}, $f_c(r_{ij})$ is a truncation function. A_i, B_i, λ_i, μ_i, ε_{ij}, χ_{ij}, β_i, n_i, m_i, δ_{ik}, ω_{ik}, c_i, d_i, h_i, R_{ij}, and S_{ij} are some correlative constants with the Si, Si—H or C system, and their values take the corresponding ones in Refs. [9–16].

In this paper, the Verlet technique [17] is used to integrate the equations of motion over time steps of $\Delta t = 0.001$ ps. In the MD simulations the NTV ensemble is taken and the temperature is controlled by the

Nose method. The following method, i.e. the method of Ref. [18], is adopted to investigate the thermal-stability of the Si—H nanotubes: (1) equilibrating the Si—H nanotubes for 20,000Δt at the temperature of 70 K; (2) increasing the temperature of the molecular systems by 2.5 K and equilibrating them at the constant temperature for 20,000Δt; (3) repeating Step 2, i.e. "heating-up", until the hydrogen atoms escape from the Si—H tubes. The following scheme is taken to simulate the axial-tension of the Si—H nanotubes: fixing the 40 Si-atoms and 60 H-atoms at one end of the nanotubes, and axially imposing tensile load on the 40 Si-atoms and 60 H-atoms at another end at the displacement step of 0.01 nm per 1000Δt. For the convenience of discussion, the similar MD simulation is also carried out for one (14,14) SWCNT (single-walled CNT) under axial-tension. The diameter of the (14,14) SWCNT is about 1.91 nm, comparable to those of the Si—H nanotubes.

3. Results and discussions

3.1 *Thermal-stability*

Figures 2 and 3, respectively, present the configuration evolvement of the Si_o—H and Si_{io}—H tubes during heating-up. In the figures, the gray spherules denote Si-atoms, and the black dots H-atoms. Figures 4 and 5 show their atomic radial distribution functions (RDFs) at different temperature. Figure 6 shows their $E-T$ curves during heating-up. Here E is the total potential-energy and T the temperature.

According to figures 2 and 3, it can be seen that some hydrogen atoms have escaped from the Si_o—H and Si_{io}—H nanotubes at 230 and 170 K, respectively, and that at 320 K only few hydrogen atoms remain on the surface of the two Si—H tubes. In fact, in the MD simulations it is found that some hydrogen atoms have began to escape from the Si_o—H and Si_{io}—H tubes at the temperature of 200 and 125 K, respectively, the amount of H-atoms escaping from the two Si—H tubes tend to saturation at the temperature above 275 and 245 K, respectively, and the Si skeletons of the two Si—H-tubes are deformed during the heating-up. This implies that the Si_o—H and Si_{io}—H tubes can stably exist only at the temperature below 200 and 125 K, respectively.

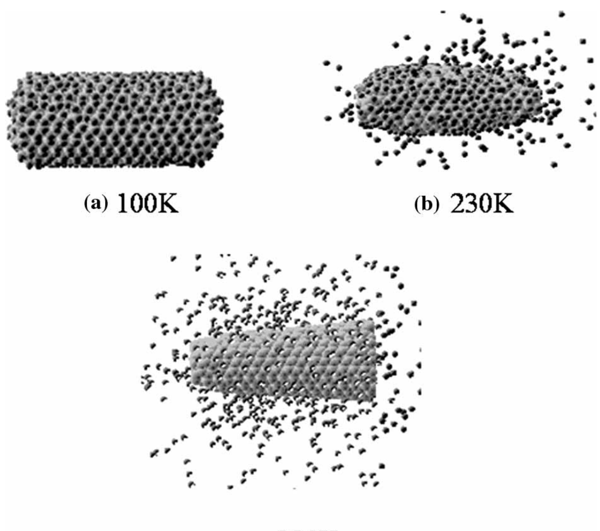
(a) 100K (b) 230K

(c) 320K

Figure 2. Configures of the Si_o—H tube during heating-up.

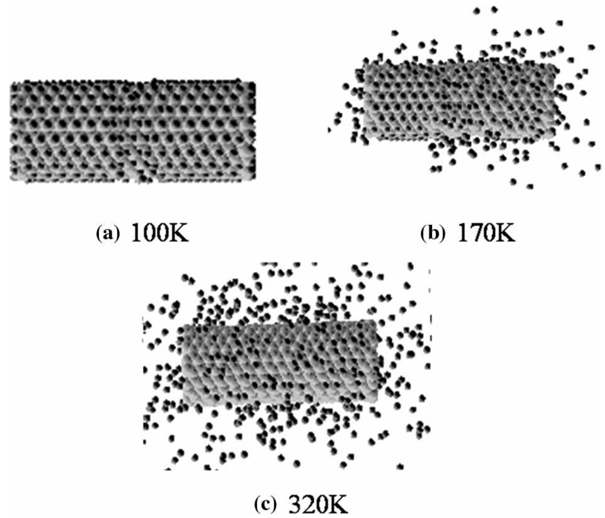
(a) 100K (b) 170K

(c) 320K

Figure 3. Configures of the Si_{io}—H tube during heating-up.

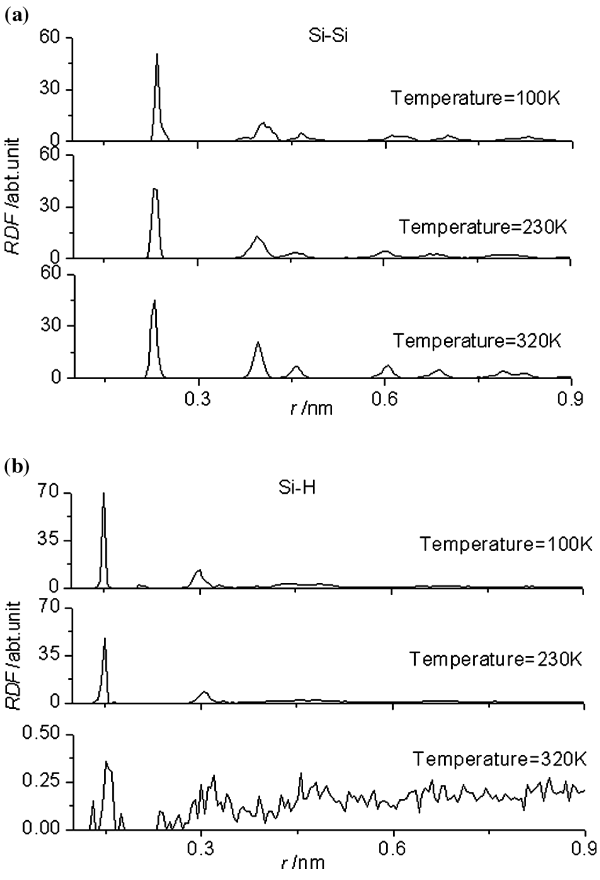

Figure 4. The RDFs of the (a) Si—Si and (b) Si—H-atoms in the Si_o—H nanotube during heating-up.

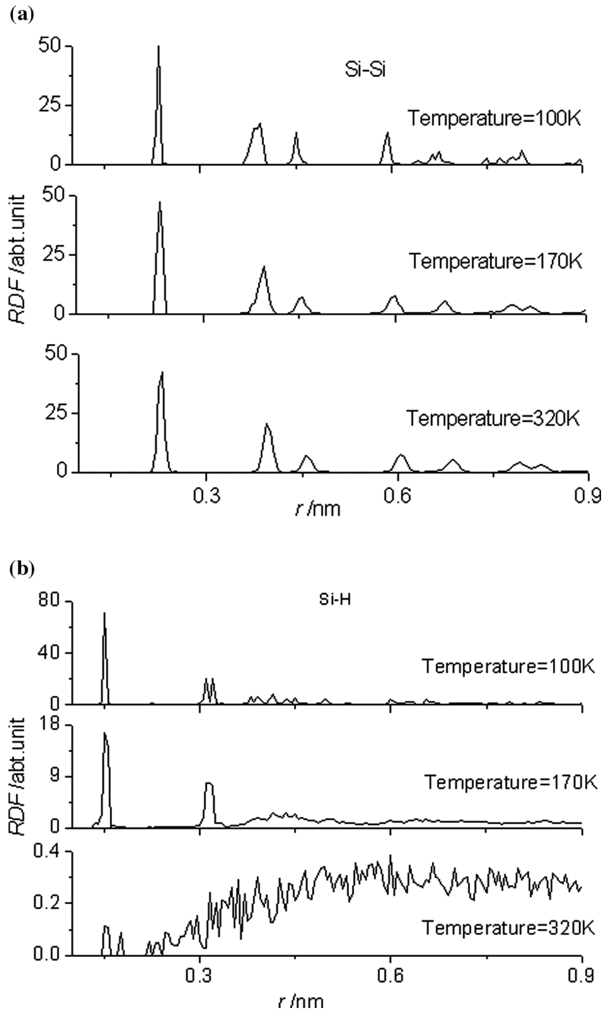

Figure 5. The RDFs of the (a) Si—Si and (b) Si—H-atoms in the $\mathrm{Si_{io}}$—H nanotube during heating-up.

From figures 4 and 5, it can be found that:

(1) During the whole heating-up, the RDFs of the Si—Si atoms for the Si—H nanotubes, as well as the peaks of the RDFs, have no significant change. The first and second peaks lie at the positions of 0.235 and 0.391 nm, respectively, and the values of 0.235 and 0.391 nm, respectively, correspond to the distance of the adjacent and sub-adjacent Si-atoms of SCS, i.e. 0.237 and 0.388 nm. This indicates that during the heating-up the Si atoms of the Si—H tubes are well-ordered and hold the diamond-like (SCS-type) structure all the time, nevertheless the Si-tubes is deformed at high temperature, see figures 2(c) and 3(c). Further observation shows that the Si skeletons of the Si—H tubes have the structure similar to the {110} planes of SCS.

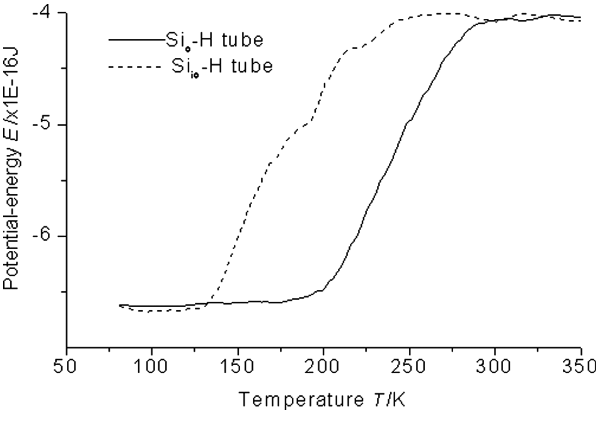

Figure 6. The energy–temperature curves of nanotubes.

(2) With the temperature increasing, the peaks of the RDFs become blunter and blunter, i.e. they become lower and wider. At the temperature of 320 K the discrete peaks almost disappear, which implies that the hydrogen atoms escaping from the Si—H nanotubes have become out-of-order.

From figure 6, it can be seen that both the $\mathrm{Si_o}$—H and $\mathrm{Si_{io}}$—H tubes have the constant potential-energy about -6.6×10^{-16} J at temperature below 200 and 125 K, respectively, their potential-energy increases with the temperature increasing during 200–275 and 125–245 K, respectively, and they again have the constant potential-energy about -4.0×10^{-16} J at temperature above 275 and 245 K, respectively. What causes the phenomenon? I think it can be attributed to the following reason: at temperature below 200 and 125 K, the $\mathrm{Si_o}$—H and $\mathrm{Si_{io}}$—H tubes have stable structure and their potential-energy hardly changes; with temperature further increasing, the Si—H bondings of the Si—H tubes begin to break, and some hydrogen atoms escape from the Si—H tubes so that their potential-energy increases; at the temperature above 275 and 245 K, almost all the hydrogen atoms escape from the two Si—H tubes, so their potential-energy again tends to another constant value, i.e. -4.0×10^{-16} J.

3.2 Tensile properties

Considering that the Si—H tubes can stably exist only at low temperature, the MD simulations of the axial-tensions of the two Si—H nanotubes and the (14,14) SWCNT are performed at the temperature of 100 K. Figure 7 shows the molecular configures of the Si—H and CNTs under tension. For clarity, in figure 7(a),(b) only the Si skeletons of the two tensile Si—H tubes are shown. Figure 8 presents their stress–strain curves. In figure 8 the arrowheads "↑" mark the moment of the three nanotubes fracturing. Here the stress is defined as $F/\pi d\delta$, F is the tensile force and δ is the wall-thickness. For the Si—H tubes, δ takes 0.31 nm [5,6], i.e. the spacing between the {110} planes of SCS; for the carbon-tube, δ takes 0.34 nm [15].

From figure 7, it can be found that the fracturing modes of the three nanotubes are different. First, both the $\mathrm{Si_o}$—H and CNTs crack in the middle, but the $\mathrm{Si_{io}}$—H tube at the loading-end; secondly, the $\mathrm{Si_o}$—H tube has obvious necking-phenomenon before fracturing, but the $\mathrm{Si_{io}}$—H and carbon-tubes donot have; thirdly, both the $\mathrm{Si_o}$—H and $\mathrm{Si_{io}}$—H tubes have the tension failure mode, but the

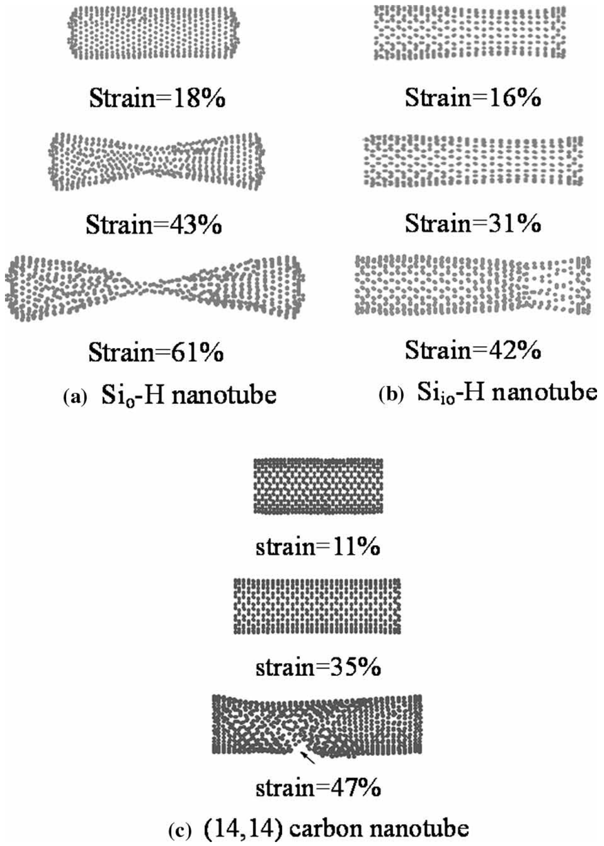

Figure 7. Tensile deformation of nanotubes.

carbon-tube has the shear failure one. Before the $\mathrm{Si_o}$—H and $\mathrm{Si_{io}}$—H tubes fracturing, a few of Si-atom chains appear at their failure positions, see figure 7(a),(b). Before fracturing, the carbon-tube cracks at a shear-angle about 60° to the tensile direction, see figure 7c. The angle of 60° just corresponds to the close-packed direction of carbon atoms on the tube-wall. In addition, before failure the Stone–Wales transformations [19], i.e. some matched heptagonal and pentagonal atomic-rings, are found at the cracking locations of the CNTs, but the Stone–Wales transformations are not found on the walls of the $\mathrm{Si_o}$—H and $\mathrm{Si_{io}}$—H tubes.

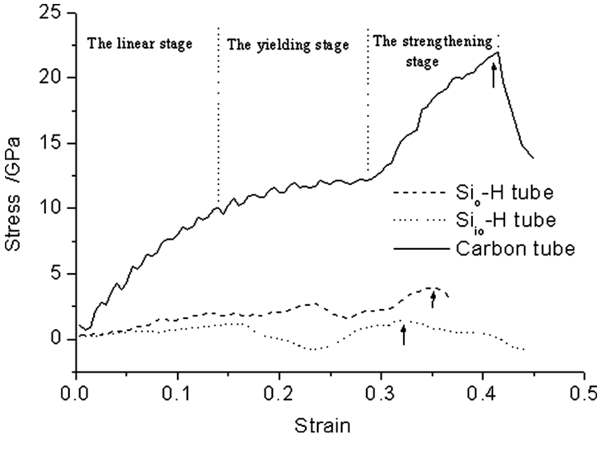

Figure 8. The stress–strain curves of three nanotubes.

From figure 8, it can be seen that:

(1) With strain increasing, the stress of the $\mathrm{Si_o}$—H and $\mathrm{Si_{io}}$—H tubes increases; after strain reaches 23 and 16%, the stress of the two Si—H tubes decreases first and then increases; when strain increase to 35 and 32%, the stress of the two Si—H tubes, respectively, reaches their maximal values, i.e. 4.0 and 1.2 GPa; after this both their stress decreases with the increase of strain.

(2) Before fracturing, the stress–strain curve of the tensile carbon-tube has an inverse-S shape and can be divided into three stages, i.e. the linear stage, the yielding stage and the strengthening stage, see figure 8. Why does the carbon-tube under tension have the strengthening stage? In Ref. [20] it was explained through the mechanical analysis of the hexagonal C atomic-units on the wall of the carbon-tube, i.e. when the tensile deformation is small, the stiffness of the carbon hexagon-unit mainly comes from the change of its bond-angles and the elongation of its C—C chemical-bonds has only small contribution to the stiffness; when the deformation is large, the carbon hexagon-unit is elongated along the tensile direction and the elongated C—C bonds have more contribution to the tensile stiffness; due to the fact that the stiffness from the elongation of C—C bonds is much larger than that from the change of bond-angles, so in the strengthening stage the stress–strain curve of the tensile carbon-tube has very large slope. In fact, due to too large deformation, in the strengthening stage the Stone–Wales transformations begin to occur on the wall of the carbon-tube.

(3) The maximal stress of material under tension is generally called as "tensile strength", and the strain corresponding to the tensile strength is called as "failure strain". The tensile strength and failure strain are often used to characterize the anti-tension and anti-deformation capability of material. Table 1 lists the tensile strength and failure strain of the three nanotubes. It is obvious that the (14,14) carbon-tube has much better anti-tension and anti-deformation capability than the two Si—H nanotubes and the $\mathrm{Si_{io}}$—H has the worst anti-tension and anti-deformation capability.

In Ref. [21], the tensile strength of CNTs is obtained through experiment. The results are within the range of 3–52 GPa. The present MD result for the (14,14) carbon-tube is 22 GPa and is very close to the ones of ref. [20], which validates the present MD simulations.

Table 1. The tensile parameters of nanotubes.

Nanotubes	*Tensile strength (GPa)*	*Failure strain*
$\mathrm{Si_o}$—H	4.0	0.35
$\mathrm{Si_{io}}$—H	1.2	0.32
Carbon	22.0	0.41

4. Conclusions

By using the Tersoff potential based MD method, the thermal-stability and tensile properties of two single-walled Si—H nanotubes are investigated. According to the simulated results, the following conclusions are obtained:

(1) The single-walled Si_o—H andSi_{io}—H nanotubes can stably exist only at the temperature lower than 200 and 125 K, respectively, and they both have the Si skeletons similar to the {110} planes of SCS.

(2) The single-walled Si_o—H and Si_{io}—H nanotubes, respectively, have the tensile strength of 4.0 and 1.2 GPa as well as the fracture strain of 0.35 and 0.32. Both their tensile strength and fracture strain are much lower than the corresponding ones of the (14,14) carbon-tube.

Acknowledgements

This research is supported by NUAA found (Y05-0103).

References

[1] H.J. Dai, J.H. Hafner, A.G. Rinzler, D.T. Colbert, R.E. Smalley. Nanotubes as nanoprobes in scanning probe microscopy. *Nature*, **384**(6605), 147 (1996).

[2] H. Shen. Creating carbon nanotube and researching into its mechanics properties by HyperChem. *Comput. Appl. Chem.*, **21**(3), 485 (2004).

[3] G. Seifert, T. Kohler, H.M. Urbassek. Tubular structures of silicon. *Phys. Rev. B*, **63**, 193409 (2001).

[4] J.W. kang. Twist of hypothetical silicon nanotubes. *Model. Simul. Mater. Sci. Eng.*, **12**, 1 (2004).

[5] D.F. Perepichka, F. Rosei. Silicon nanotubes. *Small*, **2**(1), 22 (2006).

[6] Y.H. Tang, L.Z. Pei. Research on the stability of the self-assembled silicon nanotubes. *Physics*, **35**(6), 466 (2006).

[7] L. Wang, D. Li, D. Yang. Fully exohydyrogenated Si_{60} fullerene cage. *Mol. Simul.*, **32**, 667 (2006).

[8] V. Kumar, Y. Kawazoe. Metal-encapsulated caged clusters of germanium with large gaps and different growth behavior than silicon. *Phys. Rev. Lett.*, **88**, 235504 (2002).

[9] V. Kumar, Y. Kawazoe. Metal-encapsulated fullerenelike and cubic caged clusters of silicon. *Phys. Rev. Lett.*, **87**, 045503 (2001).

[10] Hypercube Inc, *User's Manual of HyperChem® Realse 7*, Hypercube Inc., Gainesville, FL (2002).

[11] R. Fletcher, C. Reeves. Function minimization by conjugate gradients. *Comput. J.*, **7**, 149 (1964).

[12] D. Conrad, K. Scheerschmidt, U. Gösele. Molecular dynamics studies of interacting hydrogenated Si (001) surfaces. *Appl. Phys. Lett.*, **71**, 2307 (1997).

[13] J. Tersoff. New empirical model for the structural properties of silicon. *Phys. Rev. Lett.*, **56**, 632 (1986).

[14] J. Tersoff. Empirical interatomic potential for carbon, with applications to amorphous carbon. *Phys. Rev. Lett.*, **61**, 2879 (1988).

[15] J. Tersoff. Modeling solid-state chemistry: interatomic potentials for multicomponent systems. *Phys. Rev. B*, **39**, 5566 (1989).

[16] M.V. Ramana Murty, H.A. Atwater. Empirical interatomic potential for Si—H interactions. *Phys. Rev. B*, **51**, 4889 (1995).

[17] A.R. Leach. *Molecular Modeling*, pp. 316–317, Addison Wesley Longman Limited, Toronto (1996).

[18] S.G. Kim, D. Tománek. Melting the fullerenes: a molecular dynamics study. *Phys. Rev. Lett.*, **72**, 2418 (1994).

[19] P. Zhang, P.E. Lammert, V.H. Crespi. Plastic deformations of carbon nanotubes. *Phys. Rev. Lett.*, **81**, 5346 (1998).

[20] H. Shen. Molecular dynamics simulations on the melting and tensile characteristics of C, SiC and BN nanotubes. *J. Petrochemical University*, **19**(4), 60 (2006).

[21] M.F. Yu, B.S. Files, S. Arepalli, R.S. Ruoff. Tensile loading of ropes of single wall carbon nanotubes and their mechanical properties. *Phys. Rev. Lett.*, **84**, 5552 (2000).